DOI:10.28974/idojaras.2024.1.4

IDŐJÁRÁS

Quarterly Journal of the HungaroMet Hungarian Meteorological Service
Vol. 128, No. 1, January – March, 2024, pp. 59–75

Assessment and efficiency of CMIP6 models in simulation and prediction of climatic parameters of precipitation and temperature in the Samalghan basin, Iran

Zahra Zeraatkar[1], **Ali Shahidi**[2,*], and **Hadi Memarian**[3]

[1] *Department of Water Science Engineering*
University of Birjand, Birjand, Iran

[2] *Department of Water Science Engineering*
University of Birjand, Birjand, Iran

[3]*Department of Watershed Management*
Faculty of Natural Resources and Environment
University of Birjand, Birjand, Iran

**Corresponding Author e-mail: ashahidi@birjand.ac.ir*

(Manuscript received in final form December 12, 2022)

Abstract— In the present study, four global climate models MRI-ESM2-0, IPSL-CM6A-LR, CanESM5, and GFDL-ESM4 from the set of CMIP6 models are assessed to select the best model and determine the effects of climate change on temperature and precipitation parameters under three shared socioeconomic pathway scenarios (SSP1-2.6, SSP2-4.5, and SSP5-8.5) for the base period (1988–2017) and a future period (2020–2049) in the Samalghan basin. Statistical measures such as mean absolute error, root mean square error, mean bias error are applied to test the models, and the correlation coefficient is used to compare the results of the historical period of the models with the observational data of the selected stations. Taking the obtained results into account, the global climatic model IPSL-CM6A-LR is chosen to study the trend of temperature and precipitation changes in the future period under scenarios. The results of this study indicate an increasing trend of the average annual precipitation in the desied period compared to the base period for the SSP1-2.6 and SSP2-4.5 scenarios at all stations. Also, it increases in the SSP5-8.5 scenario for all stations except Besh Ghardash, Hesegah and Darkesh stations. The predictions of temperature show an increase in the minimum and maximum temperature values under all scenarios compared to the base period.

Key-words: climate change, CMIP6, SSP senarios, Samalghan basin

1. Introduction

The growth of industrial societies and increasing use of fossil fuels in recent years have led to an increase in the greenhouse gases, global warming, and melting of polar glaciers (IPCC, 2013). Climate change is one of the major threats of the 21st century. Long-term change in global average annual temperature indicates that global warming has significant effects on terrestrial ecosystems. They have lasting impacts on hydrological, agricultural, and drought cycles (*Dai*, 2011). Therefore, the assessment of the average temperature changes at the regional level as well as understanding how this parameter and its related indicators such as heat stress change at different time scales are important to implement informed decisions on economic development and climate action plans (CAP). The phenomenon of global warming is occurring according to numerous conducted studies of climate researchers around the world. Various climatic parameters such as temperature and precipitation are significantly changing in different parts of the world (*Azari et al*., 2016). Climate change is a well-documented phenomenon that is characterized by changes in climate patterns and is likely to persist (*de Oliveira et al.,* 2019). These changes, as mentioned, can have significant impacts on climatic parameters, and ultimately these changes can affect other components of a system, such as water and soil resources. This issue, therefore, highlights the importance of assessing the trend of changes in parameters such as temperature and precipitation to make well-educated management decisions for the future. One of the major sources for studying the future climate is mainly the output of atmospheric circulation models. These models are widely used to monitor and predict past and future climate changes (*He et al.,* 2019) and assess regional risk (*Khan et al*., 2020), and they can be downscaled by climate-regional techniques and models for a specific area. The output data of the Coupled Model Intercomparison Project Phase 6 (CMIP6) have recently been released (*Eyring et al.,* 2016). Previous models (e.g., CMIP3 and CMIP5) have been extensively evaluated and applied in several studies (*Maxino et al*., 2008; *McAfee et al*., 2011; *Rupp et al*., 2013; *Jiang et al*., 2015; *Bozkurt et al.,* 2018; *Almagro et al*., 2020).

The results of precipitation evaluation of previous models have indicated that the GCM outputs may significantly overestimate or underestimate the observed precipitation in different seasons (*Johnson et al*., 2011; *Gouda et al*., 2018; *Liu et al*., 2014). Several researchers (*Jia et al*., 2019; *Li et al*., 2013; *Su et al.,* 2013) analyzed a couple of CMIP5 models and obtained the same result regarding the overestimation of precipitation. *Jia et al* (2019) evaluated 33 atmospheric circulation models from the fifth report series at the Tibetan Plateau, and found that all models overestimate the precipitation, especially in spring and summer.

Also, the performance of the models may also be significantly affected by the topographic features (*Ashiq et al*., 2010). For instance, *Lv et al*. (2020) revealed that CMIP5 model simulations overestimate and underestimate precipitation in northern and southern China, respectively.

The output of the Coupled Model Intercomparison Project Phase 6 (CMIP6) are a new phase of climate models. Indeed, these models are GCMs, which have been using new scenarios (SSPs) since 2015, with a new set of concentration, emission specifications, and land cover scenarios (*Gidden et al*., 2019) to simulate the future climate of the Earth. In this phase, the combination of greenhouse gas forcing and socioeconomic trajectories has been employed for the scenarios (*Riahi et al.,* 2017). The results of recent regional evaluation studies have shown that CMIP6 models have improved and perform better than the previous models (*Rivera* and *Arnould*, 2020; *Gusain et al*., 2020). The objectives of this study are as follows:

(i) Investigating the future changes in temperature and precipitation in the Samalghan basin located in North Khorasan province by using CMIP6 models.

(ii) Evaluating the impact of climate change on these variables in three emission scenarios SSP1-2.6, SSP2-4.5, and SSP5-8.5.

The prediction of precipitation and temperature changes in future gives a proper understanding of the status of water resources in this basin and the effects of climate change on these resources in the future. Moreover, the right decisions can be made in this basin for optimal management of water resources according to these changes.

2. Material and methods

2.1. Study area

The Samalghan basin is located in the Atrak catchment in North Khorasan province with an area of 1120 km^2. This basin includes 321 km^2 mountainous area, and the rest are plains and aquifers. Its geographical coordinates are 37°24'– 37°29' E and 56°37'– 56°59' N. The highest and lowest points from the sea level are 2511 and 511 m, respectively. The geographical location of the Samalghan basin in the Atrak catchment area in North Khorasan province is shown in *Fig. 1*.

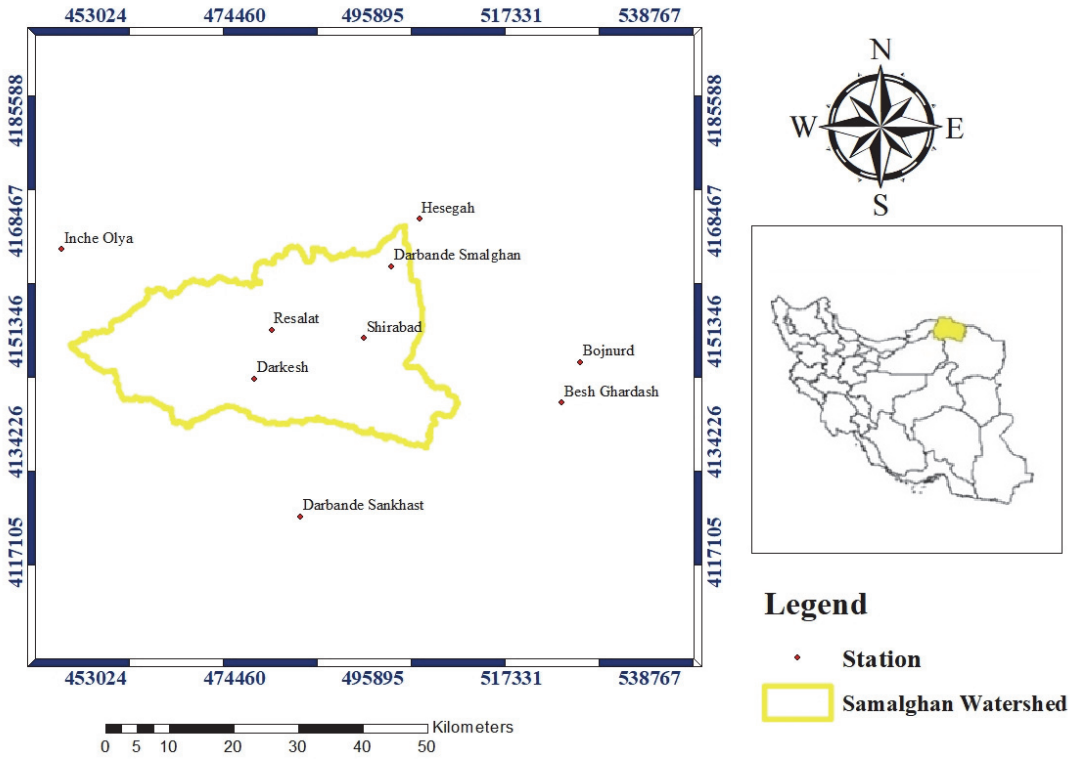

Fig. 1. Geographical location and meteorological stations of the study area.

2.2. Method

In the present study, daily data are gathered from nine stations including eight precipitation and evaporation stations (Darkesh, Shirabad, Inche Olya, Darbande Samalghan, Besh Ghardash, Darbande Sankhast, Hesegah, and Resalat) and one synoptic station (Bojnourd) during the statistical period 1988–2017. *Fig. 1* shows the location of the studied stations. The existing models and conducted research on the climate of the region are assessed to determine the trend of climate change (*Yazdandoost et al.*, 2021). After a comprehensive assessment, four global climatic models including MRI-ESM2-0, IPSL-CM6A-LR, CanESM5, and GFDL-ESM4 were selected from the set of CMIP6 models. Their specifications are presented in *Table 1*. Then, historical temperature and precipitation data of these models for the base period of 30 years (1988–2017) were prepared to test the accuracy of these models for the study area. For this purpose, the average monthly values of 30-year data of the models are compared with the average monthly values of observational data. Mean absolute error (*MAE*), root mean square error (*RMSE*), mean bias error (*MBE*), and correlation coefficient (r) are applied for comparative analysis. These statistics are computed using Eqs. (1) to (4).

$$MAE = \frac{\sum_{i=1}^{n}|O_i - P_i|}{n}, \quad (1)$$

$$RMSE = \sqrt{\frac{\sum_{i=1}^{n}(O_i - P_i)^2}{n}}, \quad (2)$$

$$MBE = \frac{\sum_{i=1}^{n} O_i - P_i}{n}, \quad (3)$$

$$r = \frac{\sum_{i=1}^{n}(O_i - \bar{O})(P_i - \bar{P})}{\sqrt{\sum_{i=1}^{n}(O_i - \bar{O})^2 \sum_{i=1}^{n}(P_i - \bar{P})^2}}, \quad (4)$$

where O_i represents the observational data values, P_i represents the predicted values by the model, i and n represent the month, and the number of months, respectively.

Table 1. List of the four CMIP6 models, utilized in the present study

Model	Institute	Country	Horizontal resolution	
			Longtitude	Latitude
CanESM5	Canadian Centre for Climate Modeling and Analysis	Canada	2.81°	2.81°
GFDL-ESM4	NOAA Geophysical Fluid Dynamics Laboratory	USA	1.25°	1°
IPSL-CM6A-LR	Institute Pierre Simon Laplace	France	2.5°	1.25°
MRI-ESM2-0	Meteorological Research Institute	Japan	1.125°	1.125°

The shared socioeconomic pathways (SSPs) scenarios are parts of a new framework for global change to provide integrated analyses of climate impacts, vulnerabilities, and adaptation policies (*Frame et al*., 2018). These scenarios enable the users organize assessments of the challenges associated with adaptation policies and possible future adjustment (*Riahi et al.*, 2017). The SSP scenarios are defined based on the five fundamental approaches of sustainable development, regional competition, inequality, growth in fossil fuels, and development based on intermediate policies (*O'Neill et al*., 2017; *Rogelj et al.,* 2018; *Estoque et al.,* 2020). These scenarios were placed in 5 categories which are known as SSP1 to SSP5. The assumptions of SSP1 include sustainable consumption, low population growth, increased energy efficiency, faster replacement of renewable energies, and more global cooperation. SSP2 assumptions represent intermediate

conditions, where the socioeconomic development is in sync with the usual conditions. The world of SSP5 is an advanced yet fossil-fueled world, where energy-intensive lifestyles are used.

The SSP1-2.6, SSP2-4.5, and SSP5-8.5 scenarios were selected from the available scenarios for two reasons:

1. Optimistic, intermediate, and pessimistic scenarios are used in the context of climate change vulnerabilities and their subsequent responses (*Warnatzsch* and *Reay*, 2019).
2. Scenario assumptions of SSP1-2.6 are very close to RCP2.6, SSP2-4.5 to RCP4.5, and SSP5-8.5 to RCP8.5, which comparison is possible with CMIP5 studies based on the results of this model.

2.3. Downscaling

Having large-scale computational cells is the main limitations of using the output of atmosphere-ocean general circulation models (AOGCM) as these cells are incompatible with hydrological models in terms of temporal and spatial accuracy. There are various methods to increase the temporal and spatial accuracy of the output of these models, which are termed downscaling. In the present study, the proportional downscaling method has been used to eliminate this limitation. In this method, monthly ratios are usually obtained for historical data series. Therefore, climate change scenarios are first created for temperature and precipitation. Then, the values of "difference" for temperature (Eq.(5)) and "ratio" for precipitation (Eq.(6)) are computed for the long-term average values of each month in the next period 2020–2049 to determine the climate change scenario in each model. The base simulation period is determined by the same model (base period 1988–2017) for each cell of the computational network (*Jones* and *Hulme*, 1996).

$$\Delta T_{\mathrm{i}} = \left(\bar{T}_{GCM,FUT,i} - \bar{T}_{GCM,base,i}\right), \tag{5}$$

$$\Delta P_i = \left(\bar{P}_{GCM,FUT,i} \Big/ \bar{P}_{GCM,base,i}\right), \tag{6}$$

which ΔT_i and ΔP_i indicate the climate change scenario associated with temperature and precipitation, respectively, for the long-term average values of 30 years per month, and $\bar{T}_{GCM,FUT,i}$ denotes the 30-year average of temperature simulated by AOGCM in the future period for each month, $\bar{T}_{GCM,base,i}$ is the 30-year average temperature simulated by AOGCM in the same period as the observational period for each month. Similarly, precipitation follows the same equation and definition of indices. After determining the climate change scenarios, the change factor method is used to apply proportional downscaling of

the data (*Tabor* and *Williams*, 2010; *Minville et al*., 2008). In the change factor method, the climate change scenarios are added to the observational values to determine the time series of the climate scenario in the future.

3. Results and discussion

3.1. Performance assessment of global climate models

To evaluate the performance of global climate models of MRI-ESM2-0, IPSL-CM6A-LR, CanESM5, and GFDL-ESM4 in generating temperature and precipitation data, the historical data series of these models are monthly compared with observational data of the base period for selected stations in the basin, and then statistical measures are determined. The results obtained from the performance of the models at these nine stations are presented in *Tables 2* and *3*. In general, the results obtained from the statistical measures indicate a relatively good performance of these models in the study area. Selecting the optimal models is based on their performance in the basin, therefore, the global climate model of the IPSL-CM6A-LR is used to assess the trend of temperature and precipitation changes in the future period under scenarios SSP1-2.6, SSP2-4.5, and SSP5-8.5 according to results.

Table 2. Values of the statistical measures in the base period for the precipitation variable at the selected stations

Station	**Model**	***MAE***	***RMSE***	***MBE***	***r***
Inche Olya	MRI-ESM2-0	0.57	0.66	-0.48	0.89
	IPSL-CM6A-LR	0.34	0.43	-0.27	0.94
	CanESM5	0.47	0.54	0.47	0.86
	GFDL-ESM4	0.61	0.73	-0.42	0.84
Resalat	MRI-ESM2-0	0.42	0.48	-0.32	0.91
	IPSL-CM6A-LR	0.20	0.24	-0.11	0.96
	CanESM5	0.63	0.75	0.63	0.82
	GFDL-ESM4	0.57	0.65	-0.26	0.75
Besh Ghardash	MRI-ESM2-0	0.58	0.65	-0.49	0.90
	IPSL-CM6A-LR	0.35	0.41	-0.27	0.94
	CanESM5	0.46	0.56	0.46	0.75
	GFDL-ESM4	0.64	0.79	-0.42	0.70
Bojnourd Synoptic	MRI-ESM2-0	0.59	0.69	-0.56	0.93
	IPSL-CM6A-LR	0.36	0.45	-0.34	0.95
	CanESM5	0.39	0.50	0.39	0.78
	GFDL-ESM4	0.66	0.81	-0.49	0.74

Table 2. Continued

Station	Model	*MAE*	*RMSE*	*MBE*	*r*
Hesegah	MRI-ESM2-0	0.38	0.46	-0.25	0.86
	IPSL-CM6A-LR	0.20	0.26	-0.03	0.92
	CanESM5	0.71	0.84	0.71	0.81
	GFDL-ESM4	0.48	0.56	-0.18	0.82
Darbande Samalghan	MRI-ESM2-0	0.48	0.54	-0.38	0.90
	IPSL-CM6A-LR	0.25	0.31	-0.16	0.95
	CanESM5	0.58	0.68	0.58	0.79
	GFDL-ESM4	0.56	0.68	-0.31	0.77
Darbande Sankhast	MRI-ESM2-0	0.61	0.72	-0.59	0.88
	IPSL-CM6A-LR	0.39	0.46	-0.37	0.95
	CanESM5	0.38	0.50	0.36	0.81
	GFDL-ESM4	0.63	0.81	-0.52	0.75
Shirabad	MRI-ESM2-0	0.31	0.37	-0.19	0.93
	IPSL-CM6A-LR	0.16	0.18	0.02	0.97
	CanESM5	0.76	0.89	0.76	0.83
	GFDL-ESM4	0.51	0.58	-0.13	0.78
Darkesh	MRI-ESM2-0	0.31	0.34	0.05	0.89
	IPSL-CM6A-LR	0.27	0.35	0.27	0.95
	CanESM5	1.00	1.19	1.00	0.80
	GFDL-ESM4	0.50	0.60	0.12	0.75

Table 3. Values of the statistical measures in the base period for the minimum and maximum temperature variables

	Station	Model	*MAE*	*RMSE*	*MBE*	*r*
Minimum temperature	Resalat	MRI-ESM2-0	3.09	3.79	-3.09	0.99
		IPSL-CM6A-LR	1.79	2.34	-1.49	0.99
		CanESM5	5.27	5.86	-1.36	0.77
		GFDL-ESM4	4.25	4.94	-2.79	0.84
	Bojnourd Synoptic	MRI-ESM2-0	2.69	3.12	-2.69	0.99
		IPSL-CM6A-LR	1.68	1.92	-1.09	0.99
		CanESM5	5.08	5.57	-0.96	0.79
		GFDL-ESM4	4.22	4.73	-2.40	0.85

Table 3. Continued

	Station	Model	*MAE*	*RMSE*	*MBE*	*r*
Maximum temperature	Resalat	MRI-ESM2-0	5.31	5.54	5.31	0.99
		IPSL-CM6A-LR	3.84	4.28	1.50	0.99
		CanESM5	8.62	10.19	-5.96	0.73
		GFDL-ESM4	5.15	5.65	-0.21	0.83
	Bojnourd Synoptic	MRI-ESM2-0	3.42	5.57	-1.12	0.99
		IPSL-CM6A-LR	2.71	3.15	2.69	0.99
		CanESM5	9.82	11.74	-8.58	0.75
		GFDL-ESM4	5.56	6.16	-2.83	0.84

3.2. The assessment of LARS-WG6 model performance in simulating basin temperature and precipitation

LARS-WG model is one of the most famous models for generating random weather data and is used to generate minimum and maximum temperature, precipitation and radiation daily in current and future climate conditions. This model is more useful than other programs due to the repetition of calculations, less need for input data and simplicity and efficiency (Kilsby et al., 2007). Also, despite the less complexity of the simulation process and input and output data, has a high ability to predict climate change (Semenov and Stratonovich, 2010). Additionally, the Long Ashton Research Station Weather Generator, version 6 (LARS-WG6) was used to dawnscale the precipitation and temperature data of the AOGCMs. Data generation by the LARS-WG6 model is performed in three stages: calibration, assessment, and meteorological data generation for the future period. The results of statistical analysis and assessment criteria show that the highest error is associated with precipitation modeling. However, the minimum and maximum temperature parameters have been modeled with high accuracy, which is consistent with the results of other studies (*Hassan et al*., 2014; *Huang et al.,* 2011; *Liu et al.,* 2011). Also, the results indicate that the LARS-WG6 model is perfectly capable of simulating the parameters of precipitation, minimum temperature and maximum temperature of the studied stations (*Table 4*). Validation of the efficiency of the model by root mean square error, mean absolute error, mean bias error, and correlation coefficient between observational data and model output in the period (1988–2017) displays that the LARS-WG6 model has the ability to model the climate of the previous period of the study basin.

Table 4. The assessment results of LARS-WG6 downscaling model in 1988–2017

Parameter	Station	*MAE*	*RMSE*	*MBE*	*r*
Precipitation	Inche Olya	2.51	3.18	-0.32	0.96
	Resalat	2.00	2.86	1.09	0.99
	Besh Ghardash	1.68	2.37	0.61	0.98
	Bojnourd Synoptic	2.09	2.52	-1.79	1.00
	Hesegah	2.29	2.89	-1.63	0.99
	Darbande Samalghan	2.97	3.63	0.63	0.97
	Darbande Sankhast	2.21	3.03	0.30	0.98
	Shirabad	2.81	3.51	-2.73	0.99
	Darkesh	2.72	3.51	-0.48	0.99
Minimum temperature	Resalat	0.17	0.19	0.00	1.00
	Bojnourd Synoptic	0.16	0.20	0.13	1.00
Maximum temperature	Resalat	0.21	0.26	0.03	1.00
	Bojnourd Synoptic	0.17	0.22	0.03	1.00

3.3. Basin climate change assessment for the 2020–2049 period in the LARS-WG6 model

The global climatic model IPSL-CM6A-LR under three scenarios (the optimistic SSP1-2.6, intermediate SSP2-4.5, and very pessimistic SSP5-8.5) are considered for the period 2020–2049 in the study area based on the results obtained from the performance of global climatic models in simulating climatic variables of temperature and precipitation on the Samalghan basin and the studied stations. Taking the capability of the LARS-WG6 model into account, the output of the IPSL-CM6A-LR model is downscaled under the relevant scenarios, and the desired parameters are predicted and compared with their values in the period 1988–2017 (*Figs. 2* and *3*).

The assessment of *Fig. 2* indicates that the average monthly precipitation in all scenarios increases in July, August, and September in all stations, whereas different results are observed in other months under these scenarios. The average annual precipitation in the desired period is increased compared to the base period for the two scenarios SSP1-2.6 and SSP2-4.5. Nonetheless, the average annual precipitation has a decreasing trend in the SSP5-8.5 scenario for Besh Ghardash, Hesegah, and Darakesh, and it has an increasing trend in other stations (*Table 5*). It should be noted, that the increase in precipitation under the three scenarios SSP1-2.6, SSP2-4.5, and SSP5-8.5 in the future period in some stations can be mainly due to different assumptions. In general, the increase in temperature in mountainous areas is mainly due to the rise in humidity which increases precipitation, therefore, it is likely that increased temperature has caused precipitation growth in the mountainous area of the Samalghan basin.

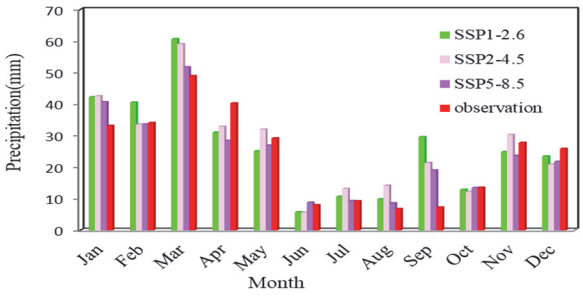

Darbande Samalghan station

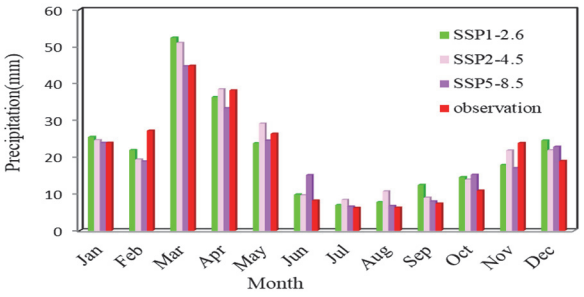

Besh Ghardash station

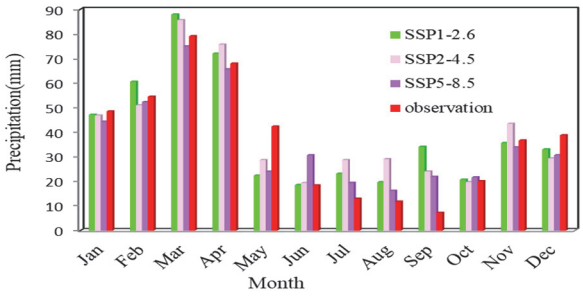

Darkesh station

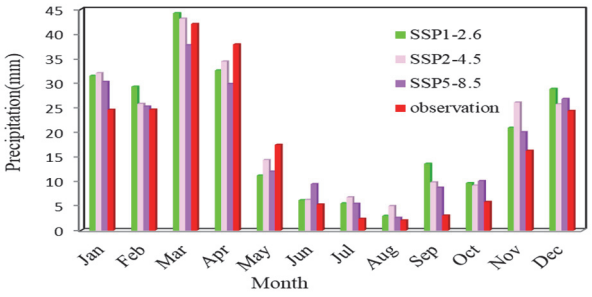

Darbande Sankhast station

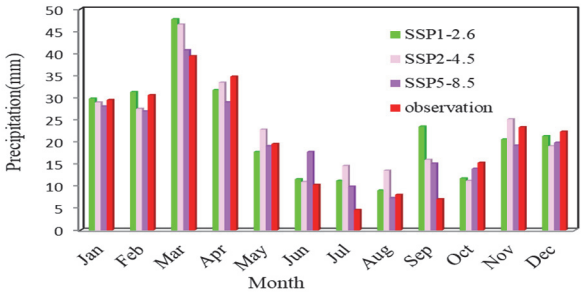

Inche Olya station

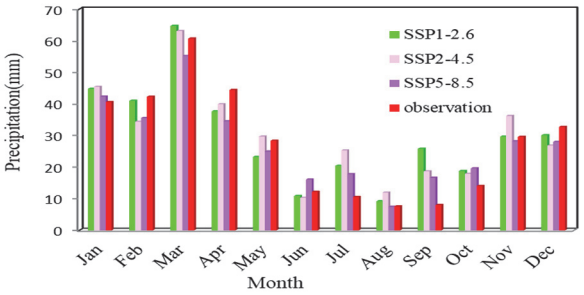

Hesegah station

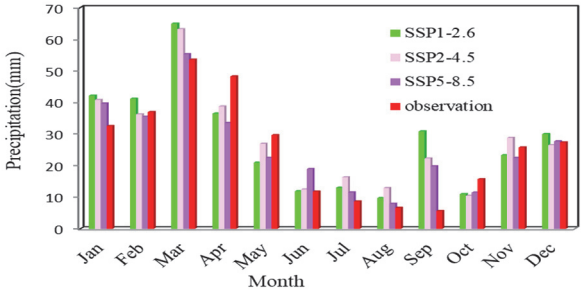

Resalat station

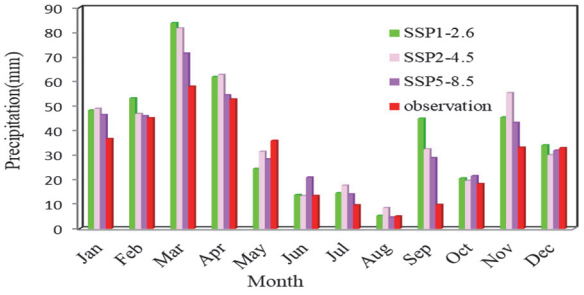

Shirabad station

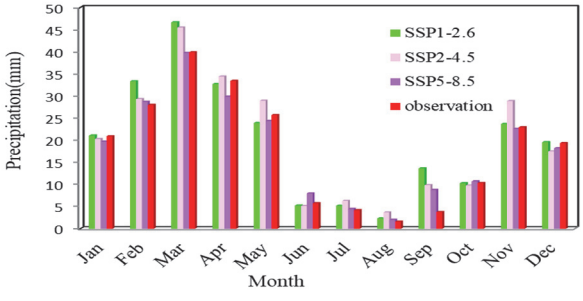

Bojnourd Synoptic station

Fig. 2. Changes in the average monthly precipitation under different scenarios for the 2020–2049 and the base period

Table 5. The average annual precipitation in the base period and under different scenarios (mm)

Station / Scenario	SSP1-2.6	SSP2-4.5	SSP5-8.5	Historical
Inche Olya	266.97	269.35	246.56	244.52
Resalat	335.38	335.38	306.29	241.98
Besh Ghardash	253.73	257.81	236.65	241.98
Bojnourd Synoptic	237.62	239.62	217.20	215.89
Hesegah	356.29	359.73	326.54	331.24
Darbande Samalghan	316.59	317.90	285.96	284.12
Darbande Sankhast	236.36	238.46	218.27	205.79
Shirabad	449.56	448.01	411.18	349.85
Darkesh	474.97	481.76	435.89	438.45

The average minimum temperature of different months in the period 2020–2049 has increased compared to the base period, however, this increase varies in different months and under various scenarios (*Fig. 3*). The highest increase occurs in September under the SSP5-8.5 scenario which are 1.69 °C and 1.62 °C for Bojnourd synoptic and Resalat stations, respectively. The lowest increase values, however, are 0.07 °C and 0.23 °C in February under the SSP1-2.6 and SSP2-4.5 scenarios, respectively for Resalat station. The lowest increase values are 0° C and 0.33 °C in January under two scenarios (SSP1-2.6 and SSP2-4.5), respectively, for Bojnourd synoptic station (*Table 6*). During this period, the values of average annual minimum temperature are 6.91 °C and 6.51 °C for Bojnourd synoptic and Resalat stations in the base period, respectively. Moreover, the average annual minimum temperature in Resalat station will increase by 10%, 12%, and 13% under scenarios SSP1-2.6, SSP2-4.5, and SSP5-8.5, respectively. Similarly, the average annual minimum temperature in Bojnourd synoptic station will increase by 11%, 14%, and 15% under scenarios SSP1-2.6, SSP2-4.5, and SSP5-8.5, respectively.

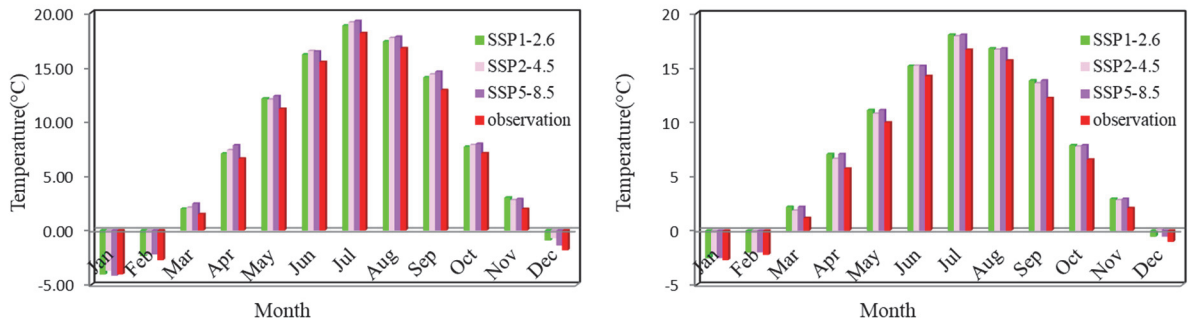

Bojnourd synoptic station Resalat station

Fig. 3. The average minimum temperature changes under different scenarios (2020-2049) and the base period.

Table 6. The minimum monthly temperature changes in the period 2020–2049 compared to the base period in °C

Station	Scenario	Jan	Feb	Mar	Apr	May	Jun	Jul	Aug	Sep	Oct	Nov	Dec
Bojnourd Synoptic	SSP1-2.6	0.00	0.38	0.50	0.47	0.94	0.69	0.70	0.62	1.18	0.60	1.04	0.91
	SSP2-4.5	0.33	0.52	0.61	0.79	0.86	1.02	0.99	0.95	1.45	0.77	0.81	1.10
	SSP5-8.5	0.00	0.52	0.98	1.22	1.17	0.96	1.12	1.06	1.69	0.87	0.91	0.43
Resalat	SSP1-2.6	0.30	0.07	0.57	0.61	0.90	0.65	0.96	0.68	1.10	1.05	0.99	0.93
	SSP2-4.5	0.64	0.23	0.69	0.92	0.82	0.96	1.26	1.01	1.37	1.22	0.75	1.13
	SSP5-8.5	0.19	0.22	1.03	1.35	1.13	0.93	1.39	1.12	1.62	1.32	0.86	0.48

The value of the average maximum temperature has increased in different months under all scenarios compared to the base period, however, this increase varies in different months and under various scenarios (*Fig. 4*). The highest increase values are 2.38 °C and 1.86 °C for Bojnourd synoptic and Resalat stations, respectively, in April, under the SSP5-8.5 scenario. The lowest increase values, however, are 0.14 °C in January under the SSP1-2.6 scenario and 0.17 °C in February under the SSP2-4.5 scenario for Resalat station. Similarly, for Bojnourd synoptic station, the lowest increase values are 0.16 °C and 0.18 °C under two scenarios SSP1-2.6 and SSP2-4.5, respectively in February (*Table 7*). In this period, the average annual maximum temperature in Bojnourd synoptic and Resalat stations are 20.03 °C and 22.65 °C in the base period, respectively**.** The average annual maximum temperature will increase 4%, 4%, and 5% under scenarios SSP1-2.6, SSP2-4.5, and SSP5-8.5, respectively, for Bojnourd synoptic station. Similarly, for Resalat station, this increase will be 3%, 4%, and 4% under scenarios SSP1-2.6, SSP2-4.5, and SSP5-8.5, respectively. The results of this study are mainly consistent with previous studies on climate change in Iran in terms of temperature variability in the future (*Soltani et al*., 2016; *Fallah-Gholhari et al.,* 2019). The results showed that temperature data had a better correlation with observational data (compared to precipitation data), which represents that temperature has a normal probability distribution, is less variable than that of the precipitation. However, precipitation is a discrete component and can be affected by various factors. Therefore, unlike temperature, precipitation does not have a pattern of significant changes in the study area, which is consistent with the results of studies by *Almazroui et al*. (2017), *Su et al.* (2016), and *Tan et al.* (2017).

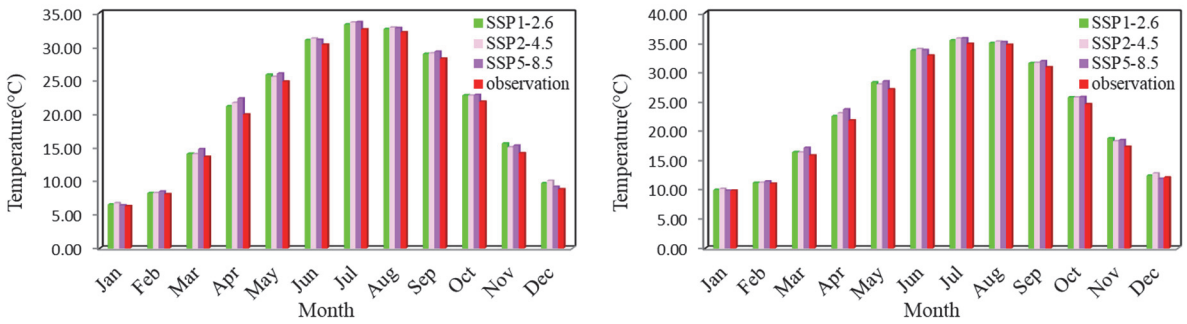

Bojnourd synoptic station Resalat station

Fig. 4. The average maximum temperature changes under different scenarios for the 2020–2049 and the base period.

Table 7. Maximum temperature changes in the period 2020–2049 compared to the base period in ° C

Station	Scenario	Jan	Feb	Mar	Apr	May	Jun	Jul	Aug	Sep	Oct	Nov	Dec
Bojnourd synoptic	SSP1-2.6	0.25	0.16	0.48	1.22	1.01	0.68	0.73	0.48	0.69	0.94	1.42	0.90
	SSP2-4.5	0.45	0.18	0.45	1.73	0.70	0.91	1.03	0.71	0.77	0.93	0.87	1.27
	SSP5-8.5	0.12	0.40	1.18	2.38	1.19	0.73	1.08	0.66	1.03	1.00	1.14	0.37
Resalat	SSP1-2.6	0.14	0.16	0.56	0.71	1.19	0.90	0.60	0.30	0.71	1.17	1.43	0.33
	SSP2-4.5	0.34	0.17	0.53	1.21	0.87	1.14	0.90	0.54	0.78	1.15	0.95	0.70
	SSP5-8.5	0.01	0.39	1.27	1.86	1.37	0.95	0.95	0.48	1.06	1.23	1.14	0

4. Conclusions

In the present study, models of the Coupled Model Intercomparison Project Phase 6 (CMIP6) are applied to assess changes in climate parameters in arid regions, which are more sensitive to climate change. Nowadays, the importance of determining the appropriate model that can make future predictions increases with the growth of research on climate change. The results showed that temperature data had a better correlation with observational data, and precipitation is a discrete component. Therefore, unlike temperature, precipitation does not have a pattern of significant changes in the study area. Precipitation will increase in the future period of 2020–2049 under three scenarios (SSP1-2.6, SSP2-4.5, and SSP5-8.5) in July, August, and September at all stations according to the results. This increase can be due to increased humidity caused by rising temperatures in the mountainous areas under the three scenarios SSP1-2.6, SSP2-4.5, and SSP5-8.5

in the future period at some stations. In general, the average precipitation will decrease as we move towards the final years of the future period in all scenarios, and this decrease occurs more in the SSP5-8.5 scenario than in the other two scenarios. Moreover, the temperature trend in the future period has increased under all scenarios compared to the base period. The highest temperature increase is in September under the SSP5-8.5 scenario, while the lowest temperature increase is in February and January under the SSP1-2.6 and SSP2-4.5 scenarios for Bojnourd synoptic and Resalat stations, respectively. Also, the highest maximum temperature increase occurs in April under the SSP5-8.5 scenario and the lowest maximum temperature increase occurs in January under the SSP1-2.6 scenario and in February under the SSP2-4.5 scenario for Resalat station. Similarly, it occurs in February under the SSP1-2.6 and SSP2-4.5 scenarios for Bojnourd synoptic station. The results of this study recommend considering temperature variability in water resources management, especially in agricultural section to avoid the possible negative effects of climate change in the region.

References

Almazroui, M., Islam, M.N., Saeed, F., Alkhalaf, A.K., and *Dambul, R.,* 2017: Assessing the robustness and uncertainties of projected changes in temperature and precipitation in AR5 Global Climate Models over the Arabian Peninsula, *Atmosph. Res. 194*, 202–213. https://doi.org/10.1016/j.atmosres.2017.05.005

Almagro, A., Oliveira, P.T.S., Rosolem, R., Hagemann, S., and *Nobre, C.A.,* 2020: Performance evaluation of Eta/HadGEM2-ES and Eta/MIROC5 precipitation simulations over Brazil. *Atmosph. Res. 244*, 105053. https://doi.org/10.1016/j.atmosres.2020.105053

Ashiq, M.W., Zhao, C., Ni, J., and *Akhtar, M.,* 2010: GIS-based high-resolution spatial interpolation of precipitation in mountain–plain areas of Upper Pakistan for regional climate change impact studies. Theoretical and *Appl. Climatol. 99*, 239–253. https://doi.org/10.1007/s00704-009-0140-y

Azari, M., Moradi, H.R., Saghafian, B., and *Faramarzi, M.,* 2016: Climate change impacts on streamflow and sediment yield in the North of Iran. *Hydrol. Sci. J. 61*, 123–133. https://doi.org/10.1080/02626667.2014.967695

Bozkurt, D., Rojas, M., Boisier, J.P., and *Valdivieso, J.,* 2018: Projected hydroclimate changes over Andean basins in central Chile from downscaled CMIP5 models under the low and high emission scenarios. *Climatic Change*, *150*, 131–147. https://doi.org/10.1007/s10584-018-2246-7

Dai, A., 2011: Drought under global warming: a review. Wiley Interdisciplinary Reviews: *Climate Change*, *2*, 45–65. https://doi.org/10.1002/wcc.81

de Oliveira, V.A., de Mello, C.R., Beskow, S., Viola, M.R., and *Srinivasan, R.,* 2019: Modeling the effects of climate change on hydrology and sediment load in a headwater basin in the Brazilian Cerrado biome. *Ecol. Engineer. 133*, 20–31.

Estoque, R.C., Ooba, M., Togawa, T., and *Hijioka, Y.,* 2020: Projected land-use changes in the Shared Socioeconomic Pathways: Insights and implications. *Ambio*, *49*, 1972–1981. https://doi.org/10.1007/s13280-020-01338-4

Eyring, V., Bony, S., Meehl, G. A., Senior, C. A., Stevens, B., Stouffer, R. J., and Taylor, K. E. 2016. Overview of the Coupled Model Intercomparison Project Phase 6 (CMIP6) experimental design and organization. *Geoscientific Model Development, 9, 1937-1958*

Fallah-Ghalhari, G., Shakeri, F., and *Dadashi-Roudbari, A.,* 2019: Impacts of climate changes on the maximum and minimum temperature in Iran. *Theor. Appl. Climat. 138*, 1539–1562. https://doi.org/10.1007/s00704-019-02906-9

Frame, B., Lawrence, J., Ausseil, A.G., Reisinger, A., and *Daigneault, A.,* 2018: Adapting global shared socio-economic pathways for national and local scenarios. *Climate Risk Manage. 21*, 39–51. https://doi.org/10.1016/j.crm.2018.05.001

Gidden, M.J., Riahi, K., Smith, S.J., Fujimori, S., Luderer, G., Kriegler, E., ... and *Takahashi, K.,* 2019: Global emissions pathways under different socioeconomic scenarios for use in CMIP6: a dataset of harmonized emissions trajectories through the end of the century. *Geosci. Model Develop 12*, 1443–1475. https://doi.org/10.5194/gmd-12-1443-2019

Gouda, K.C., Nahak, S., and *Goswami, P.,* 2018: Evaluation of a GCM in seasonal forecasting of extreme rainfall events over continental India. *Weather Climate Extrem. 21*, 10–16. https://doi.org/10.1016/j.wace.2018.05.001

Gusain, A., Ghosh, S., and *Karmakar, S.,* 2020: Added value of CMIP6 over CMIP5 models in simulating Indian summer monsoon rainfall. *Atmosph. Res. 232*, 104680. https://doi.org/10.1016/j.atmosres.2019.104680.

Hassan, Z., Shamsudin, S., and *Harun, S.,* 2014: Application of SDSM and LARS-WG for simulating and downscaling of rainfall and temperature. *Theor. Appl. Climatol. 116*, 243–257. https://doi.org/10.1007/s00704-013-0951-8

Huang, J., Zhang, J., Zhang, Z., Xu, C., Wang, B., and *Yao, J.,* 2011: Estimation of future precipitation change in the Yangtze River basin by using statistical downscaling method. *Stoch. Environ. Res. Risk Assess. 25*, 781–792. https://doi.org/10.1007/s00477-010-0441-9

He, S., Yang, J., Bao, Q., Wang, L., and *Wang, B*., 2019: Fidelity of the observational/reanalysis datasets and global climate models in representation of extreme precipitation in East China. *J.Climate 32*, 195–212. https://doi.org/10.1175/JCLI-D-18-0104.1

IPCC, 2013: Climate Change. 2013. The Physical Science Basis. Contribution of Working Group I to the Fifth Assessment Report of the Intergovernmental Panel on Climate Change. Cambridge University Press, Cambridge and New York.

Jones, P.D. and *Hulme, M.,* 1996: Calculating regional climatic times series for temperature and precipitation: methods and illustrations. *Int. J. Climatology 16*, 361–377. https://doi.org/10.1002/(SICI)1097-0088(199604)16:4<361::AID-JOC53>3.0.CO;2-F

Jia, K., Ruan, Y., Yang, Y., and *Zhang, C.,* 2019: Assessing the performance of CMIP5 global climate models for simulating future precipitation change in the Tibetan Plateau. *Water*, *11*, 1771. https://doi.org/10.3390/w11091771.

Jiang, Z., Li, W., Xu, J., and *Li, L.,* 2015: Extreme precipitation indices over China in CMIP5 models. Part I: Model evaluation. *Journal of Climate*, *28*, 8603-8619. https://doi.org/10.1175/JCLI-D-15-0099.1

Johnson, F., Westra, S., Sharma, A., and *Pitman, A.J.,* 2011: An assessment of GCM skill in simulating persistence across multiple time scales. *J. of Climate*, *24*, 3609–3623. https://doi.org/10.1175/2011JCLI3732.1

Khan, A. J., Koch, M., and *Tahir, A. A.,* 2020: Impacts of climate change on the water availability, seasonality and extremes in the Upper Indus Basin (UIB). *Sustainability 12*, 1283. https://doi.org/10.3390/su12041283

Kilsby C. G. Jones P. D. Burton A. Ford A. C. Fowler H. J. Harpham C. James P. Smith A. and Wilby R. L. 2007. A daily weather generator for use in climate change studies. *Environmental Modelling & Software*. 22, 1705-1719.

Liu, Z., Mehran, A., Phillips, T.J., and *AghaKouchak, A.,* 2014: Seasonal and regional biases in CMIP5 precipitation simulations. *Climate Res. 60*, 35–50. https://doi.org/10.3354/cr01221

Liu, L., Liu, Z., Ren, X., Fischer, T., and *Xu, Y.,* 2011: Hydrological impacts of climate change in the Yellow River Basin for the 21st century using hydrological model and statistical downscaling model. *Quaternary Int. 244*, 211–220. https://doi. org/10.1016/j.quaint.2010.12.001

Lv, Y., Guo, J., Yim, S.H.L., Yun, Y., Yin, J., Liu, L., ... and *Chen, D.,* 2020: Towards understanding multi-model precipitation predictions from CMIP5 based on China hourly merged precipitation analysis data. *Atmosph. Res. 231*, 104671. https://doi.org/10.1016/j.atmosres.2019.104671

Li, Z., Wei, Z.G., Lv, S.H., Han, B., Ao, Y.H., and *Chen, H.,* 2013: Verifications of surface air temperature and precipitation from CMIP5 model in Northern Hemisphere and Qinghai-Xizang Plateau. *Plateau Meteorol*. *32*, 921.

Maxino, C.C., McAvaney, B.J., Pitman, A.J., and *Perkins, S.E.*, 2008: Ranking the AR4 climate models over the Murray-Darling Basin using simulated maximum temperature, minimum temperature and precipitation. *Int. J. Climatol. 28*, 1097–1112. https://doi.org/10.1002/joc.1612

McAfee, S.A., Russell, J.L., and *Goodman, P.J.,* 2011: Evaluating IPCC AR4 cool-season precipitation simulations and projections for impacts assessment over North America. *Climate Dynam. 37*, 2271–2287. https://doi.org/10.1007/s00382-011-1136-8

Minville, M., Brissette, F., and *Leconte, R.,* 2008: Uncertainty of the impact of climate change on the hydrology of a nordic watershed. *J. Hydrology 358*, 70–83. https://doi.org/10.1016/j.jhydrol.2008.05.033

O'Neill, B.C., Kriegler, E., Ebi, K.L., Kemp-Benedict, E., Riahi, K., Rothman, D.S., ... and *Solecki, W.,* 2017: The roads ahead: Narratives for shared socioeconomic pathways describing world futures in the 21st century. *Global Environmental Change 42*, 169–180. https://doi.org/10.1016/j.gloenvcha.2015.01.004

Rivera, J.A., and *Arnould, G.,* 2020: Evaluation of the ability of CMIP6 models to simulate precipitation over Southwestern South America: Climatic features and long-term trends (1901–2014). *Atmosph. Res. 241*, 104953. https://doi.org/10.1016/j.atmosres.2020.104953

Riahi, K., Van Vuuren, D.P., Kriegler, E., Edmonds, J., O'neill, B.C., Fujimori, S., ... and *Tavoni, M.,* 2017: The shared socioeconomic pathways and their energy, land use, and greenhouse gas emissions implications: an overview. *Glob. Environ. Change 42*, 153–168. https://doi.org/10.1016/j.gloenvcha.2016.05.009

Rupp, D.E., Abatzoglou, J.T., Hegewisch, K.C., and Mote, *P.W.,* 2013: Evaluation of CMIP5 20th century climate simulations for the Pacific Northwest USA. *J. Geophys Res: Atmospheres 118*, 10,884–10,906. https://doi.org/10.1002/jgrd.50843

Rogelj, J., Popp, A., Calvin, K.V., Luderer, G., Emmerling, J., Gernaat, D., ... and *Tavoni, M.,* 2018: Scenarios towards limiting global mean temperature increase below 1.5 C. *Nat. Climate Change 8*, 325–332. https://doi.org/10.1038/s41558-018-0091-3

Semenov M. A. and Stratonovitch P. 2010. Use of multi-model ensembles from global climate models for assessment of climate change impacts. *Climate research*. 41, 1- 14.

Soltani, M., Laux, P., Kunstmann, H., Stan, K., Sohrabi, M.M., Molanejad, M., ... and *Martin, M.V.,* 2016: Assessment of climate variations in temperature and precipitation extreme events over Iran. *Theor. Appl. Climatol. 126*, 775–795. https://doi.org/10.1007/s00704-015-1609-5

Su, F., Duan, X., Chen, D., Hao, Z., and *Cuo, L.,* 2013: Evaluation of the global climate models in the CMIP5 over the Tibetan Plateau. *J. Climate 26*, 3187–3208. https://doi.org/10.1175/JCLI-D-12-00321.1

Su, B., Huang, J., Gemmer, M., Jian, D., Tao, H., Jiang, T., and *Zhao, C.,* 2016: Statistical downscaling of CMIP5 multi-model ensemble for projected changes of climate in the Indus River Basin. *Atmos. Res 178–179*, 138–149. https://doi.org/10.1016/j.atmosres.2016.03.023

Tan, M.L., Ibrahim, A.L., Yusop, Z., Chua, V.P., and *Chan, N.W.,* 2017: Climate change impacts under CMIP5 RCP scenarios on water resources of the Kelantan River Basin, Malaysia. *Atmos. Res 189*, 1–10. https://doi.org/10.1016/j.atmosres.2017.01.008

Tabor, K., and *Willams, J.,* 2010: Global downscaled climate projections for assessing the conservation impacts of climate change. *Ecol. Appl. 20*, 554–565. https://doi.org/10.1890/09-0173.1

Warnatzsch, E.A. and *Reay, D.S.,* 2019: Temperature and precipitation change in Malawi: Evaluation of CORDEX-Africa climate simulations for climate change impact assessments and adaptation planning. *Sci. Total Environ. 654*, 378–392. https://doi.org/10.1016/j.scitotenv.2018.11.098

Yazdandoost, F., Moradian, S., Izadi, A., and *Aghakouchak, A.,* 2021: Evaluation of CMIP6 precipitation simulations across different climatic zones: Uncertainty and model intercomparison. *Atmosph. Res. 250*, 105369. https://doi.org/10.1016/j.atmosres.2020.105369